ELSEVIER

Composites: Part A 32 (2001) 1133–1142

composites
Part A: applied science and manufacturing

www.elsevier.com/locate/compositesa

Affordable processing of thick section and integral multi-functional composites

U.K. Vaidya*, A. Abraham, S. Bhide

Department of Mechanical Engineering and Applied Mechanics (MEAM), Composites Research Laboratory, North Dakota State University (NDSU), Fargo, ND 58105 USA

Received 29 May 2000; revised 20 December 2000; accepted 22 December 2000

Abstract

The use of multi-functional integral armor is of current interest in armored vehicles and military carriers. In the present study, thick-section laminated composites and multi-layered integrated composites have been processed/manufactured with the aim of providing multi-functionality including easy reparability, quick deployment, enhanced ballistic damage and fire protection, as well as lightweight advantages. The design of an integral armor utilizes a combination of thick-section structural composite, ceramic tiles, resilient rubber, fire retardant laminate liner and a composite durability cover. Processing techniques such as automated fiber placement and/or autoclave molding are traditionally used to process dissimilar multi-layered structure, but prove to be expensive.

This work focuses on emerging cost-effective liquid molding processes such as vacuum assisted resin transfer/infusion molding (VARTM) for the production of thick-section and integral armor parts (up to 50 mm thick). While thick-section composites have applications in a variety of structures including armored vehicles, marine bodies, civil infrastructure, etc. in the present work they refer to the structural laminate within the integral armor. The processing steps of thick-section composite panels and integral armor have been presented. The integrity of the interfaces has been evaluated through scanning electron microscopy (SEM). Representative results on static and dynamic response (high strain rate, HSR and ballistic impact) of the VARTM processed thick-section composite panels are presented. Wherever applicable, comparisons are made to conventional closed-mold resin transfer molding (CMRTM). Process sensing by way of flow and cure monitoring of the resin in the fiber perform has been conducted using embedded direct current (DC)-based sensors in the thick-section preform and integral armor interfaces. The feasibility of cost-effective VARTM for producing thick-section composites and integral armor has been demonstrated.

Keywords: Scanning electron microscopy; E. Resin transfer moulding (RTM)

1. Introduction

Light weight ground combat vehicles, marine bodies and aircraft structures using advanced fabric/textile composites and/or layered material architecture are of importance because they offer improved deployability, survivability, and agility [1,2]. Components such as armored tank hull, crew capsule, rear engine bulkhead, ramp and sidewalls, etc. utilize composites with various types of fabric architectures and resin compositions (for example, S-2 glass, vinyl ester, epoxy and phenolic resins) as monocoque or sandwich hybrid constructions [1–5]. In recent years, affordability is of high interest in manufacturing composite and integrated structures. Promising techniques such as closed-mold resin transfer molding (CMRTM) and vacuum assisted resin transfer/infusion molding (VARTM) have emerged as alternative techniques in comparison to autoclave and/or automated fiber placement (AFP). The application of these processing techniques to thick-section and multi-layered structure lends itself to significant potential cost-savings.

1.1. Integral armor

A composite integral armor is designed to provide multi-interface, multi-functional capability, easy reparability, quick deployment, enhanced ballistic damage protection, and lightweight advantages. The design of the integral armor adopted in the present work is schematically illustrated in Fig. 1. The components of the armor are: (a) *Durability cover* for outer shell comprising S2-glass reinforcement (approximately 4 mm thick). (b) *Ceramic tiles* for ballistic protection of approximately 17 mm thickness. (c) *Ethylene propylene diene monomer* (EPDM) *rubber* for multi-hit damage tolerance (approximately 2–3 mm thick). (d) *Thick section composite structural*

* Corresponding author. Tel.: +1-701-231-6493; fax: +1-701-231-8913.
E-mail address: uday_vaidya@ndsu.nodak.edu (U.K. Vaidya).

1359-835X/01/$ - see front matter
PII: S1359-835X(01)00033-1

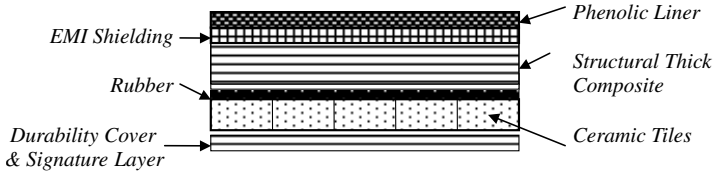

Fig. 1. Schematic of integral armor.

laminate which is the primary structural load bearing component, 20–25 mm thick comprising S2-glass reinforcement with vinyl ester or epoxy resin matrix. (e) *Electromagnetic interference* (EMI) *mesh* for electromagnetic shielding. (f) A *Phenolic laminate liner* for flammability protection (S2-glass/phenolic reinforcement)

In the current study, VARTM and CMRTM have been utilized in the manufacturing of the structural load bearing composite laminate (referred to as the thick-section composite) and the integral armor comprising the various layers described above. The microstructure of the resulting laminates, as well as the integral armor has been studied. The flow and cure monitoring of the liquid resin in the processing of thick-section composites, and the integral armor has been evaluated using a DC-based sensing technique [6–9]. Representative static and dynamic (high strain rate and ballistic impact) test results for the thick-section structural laminate accompanied by ultrasonic C-scan studies have been presented.

1.2. Vacuum assisted resin infusion/transfer molding

Vacuum assisted resin infusion/transfer molding (VARTM) is of interest in low-cost innovative developments, as it uses single-sided tooling and vacuum-bag technology. It is an emerging manufacturing technique that holds promise as an affordable alternative to traditional autoclave molding and AFP for producing large-scale structural parts. In VARTM, the preform is laid on a single sided tool, which is then bagged along with the infusion and vacuum lines. The resin is infused through the preform, which causes wetting in the in-plane and transverse directions of the preform. This process is proving to be a very attractive alternative to spray-up or impregnation methods, and it is far less expensive than conventional manufacturing methods. Large structural parts with high fiber volume fractions can be produced rapidly. Other advantages of CMRTM and VARTM are low process volatile emissions, high fiber-to-resin ratios and good process repeatability [3,10].

2. Processing of thick composite panels

Thick-section composite panels were manufactured from S2-glass/vinyl ester epoxy resin by two methods VARTM

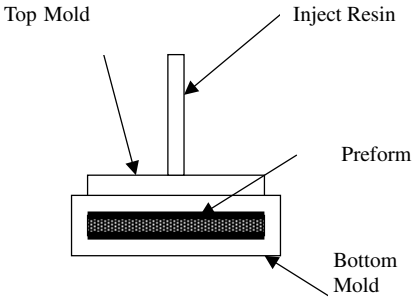

a)

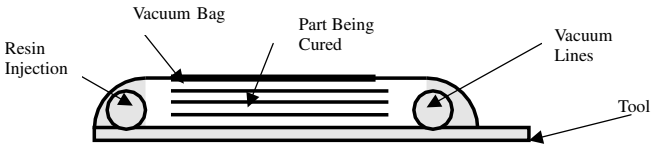

b)

Fig. 2. Schematic of the CMRTM and VARTM processes.

and CMRTM. Fig. 2(a) and (b) provide a schematic illustration of the VARTM and the CMRTM processes. Forty-five layers (plies) of Owens Corning S2-glass fabric-twill weave architecture (0.58 mm/ply) were used to obtain the thick-section composite laminate. Dow Derakane Vinyl Ester 350 (VE350) resin system was used. The resin constituents added to the VE350 system were 6% solution of Cobalt Naphthenate/Octoate (CoNap/Oct) promoter, methyl ethyl ketone peroxide (MEKP) catalyst and dimethylaniline (DMA) accelerator, and 2,4-pentanedione (acetylacetone).

VARTM laminates. Forty-five layers of S2-glass preform were stacked on an aluminum caul plate. A porous teflon layer and a highly permeable nylon net (referred to as 'distribution mesh') were laid on top of the preform. Spiral tubing was used to channel the resin through the perform. Following the lay-up and bagging procedures, the preform was debulked for 3 h.

CMRTM laminates. A Liquid Control Corporation Positron compact variable ratio (CVR), twin flow metering, mixing and dispensing unit, in conjunction with a pneumatic press 0.41 MPa was used. A disposable mixing head was used to inject resin into the mold at its center at 0.17 MPa. The mold measured 762 mm × 863 mm × 45 mm. Spacers were used within the mold to obtain the laminate of 20 mm thickness. The typical finished dimensions of the laminates were 711 mm × 609 mm × 20 mm in both cases.

3. Experimental: thick-section composites

The performance of the laminates was investigated for several loading situations. (a) *Static compression tests*. Samples of dimensions 38 mm × 25 mm × 20 mm were adopted for compression [10,11] and HSR impact testing. A 50,000 kg Mechanical Testing System (MTS) was used to conduct compression testing of the sample to failure. (b) *High strain rate impact tests*. For HSR impact testing, a compression Split Hopkinson Pressure Bar (SHPB) setup equipped with 38.1 mm diameter bar was used [12,13]. The lengths of incident and transmission bars were 1.52 m and that of striker bar was 0.3 m. These samples were subjected to high strain rate impact loading in the in-plane direction. (c) *Ballistic impact testing*. Laminates of 304 mm × 304 mm × 20 mm were subjected to ballistic testing in a light gas gun with a 76.2 mm barrel with sabo-assisted 50 caliber fragmented simulated projectile (FSP) [14,15]. Impact velocities of 400–450 m/s were adopted, which represents the ballistic limit for the 20 mm thick S2-glass/VE laminates.

4. Results and discussion

4.1. CMRTM vs VARTM processed thick section laminates

Microstructure. The microstructure of the VARTM route processed composites was compared to the laminates processed by CMRTM. Several microstructural differences were observed for the two processes. The extent of fiber compaction is greater in the CMRTM composites in comparison to the VARTM composites as shown in Fig. 3(a). This is attributed to the positive pressure of 0.41 MPa from the compaction provided by the pneumatic press, accompanied by 0.09 MPa or vacuum applied at the vents, in comparison to the vacuum pressure of 0.09 MPa adopted in the VARTM operation. The size of the matrix

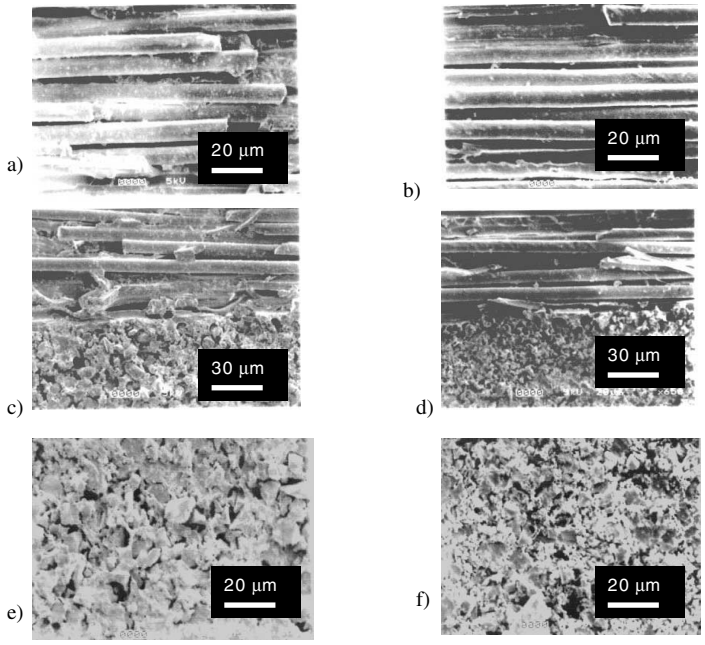

Fig. 3. CMRTM and VARTM composite. (a,b) Extent of fiber compaction, (c,d) Wetting characteristics and (e,f) Size of the matrix agglomerates.

Table 1
Quantification of CMRTM and VARTM microstructure

	CMRTM	VARTM
Crimp angle	15°	17.5°
Matrix agglomerate size (μm^2)	1.43	3.4
Average no. of agglomerates	39	34
Yarn height (mm)	0.4	0.6

agglomerates for the CMRTM laminates was smaller ($<1.43\ \mu m^2$) as compared to VARTM where the average matrix agglomerate size was 3.4 μm^2) as shown in Fig. 3(b). The wetting characteristics were observed to be different as shown in Fig. 3(c). In the VARTM process, tow level wetting was noted, with several dry filaments within the tow (as resin flows around the tows), while in the CMRTM the pressure from the press aided in wet-out of the tows at the filament level.

The above observations were quantitatively studied by measuring parameters such as fiber waviness (crimp angle), yarn height, major axis, average number of matrix agglomerates, and the size of matrix agglomerates as measured with the aid of scanning electron microscopy (SEM). Table 1 summarizes these results.

Static compression and high strain rate impact response. Samples were subjected to in-plane loading (along the fiber direction) for static and high strain rate impact testing. The average static compression strength was determined to be 236 MPa for the VARTM samples, and 250 MPa for the CMRTM samples. The increase in compression strength of the CMRTM samples may be attributed to the localized microstructure features from variations reported in Table 1. The CMRTM samples had higher compaction, smaller matrix agglomerates (intimate wet-out) and smaller crimp angles as compared to the VARTM samples. In all the cases, the samples *failed in two ways*. In some samples, the formation of kink-bands and shear failure occurred across their thickness [13]. Failure was through collective progression of microbuckling of the fibers in the single shear plane as illustrated in Fig. 4(a). In some instances, failure initiated at two edges of the sample and forking was observed around the mid-plane as shown in Fig. 4(b).

Table 2
Comparison of failure strength (MPa) and strain (mm/mm) of CMRTM and VARTM laminates

	Static	HSR: 338 (s)[a]	HSR: 422 (s)[a]	HSR: 507 (s)[a]
Strength (MPa)				
VARTM	234	310	361	322
CMRTM	250	250	298	346
Strain (mm/mm)				
VARTM	1.86	2.55	1.83	1.94
CMRTM	2.87	2.01	2.71	2.28

[a] Strain rates adopted in testing.

The high strain rate impact results for both CMRTM and VARTM samples indicate an increase in dynamic compressive peak stress as compared to the static case. The characteristics of failure were similar to that observed under the static loading case, where damage initiates from the loading face, as a shear crack through collective micro buckling of the fibers a single shear plane or through forking. In a few of these samples, the samples were seen to delaminate along a weak location along the crimp. Table 2 summarizes the values of the static and high strain rate impact test results from CMRTM vs. VARTM processed panels.

Ballistic impact tests. The ballistic impact damage profile was seen to be fairly independent of the processing method, i.e. CMRTM or VARTM. Nearing ballistic limit, i.e. approximately 425 m/s, the CMRTM and the VARTM laminates exhibited shear plugging of the fibers on the impact side, and extended delamination damage towards the back face (Fig. 5). The spread of delamination is a conical zone, where the maximum delamination spread occurs in the inner layers nearing the back face of the laminate. Ultrasonic C-scans were obtained for different

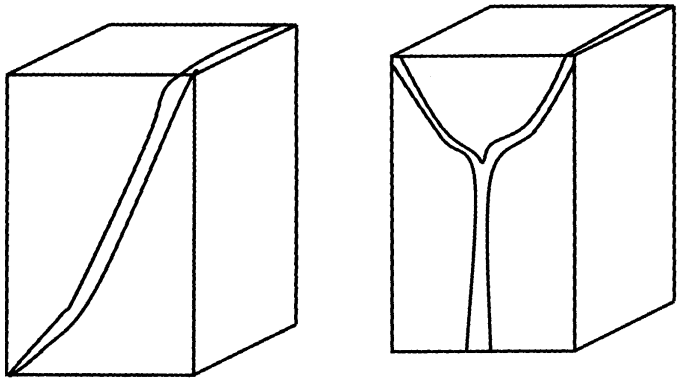

a) b)

Fig. 4. Failure of S2-glass/VE in compression. (a) Single plane of fracture, and (b) forking.

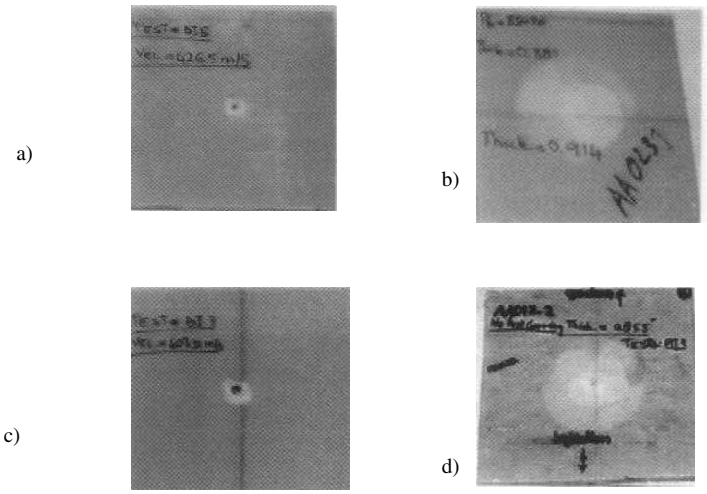

Fig. 5. Ballistic impact damage in (a,b) CMRTM (a — impact face, b — back side), and (c,d) (c — impact face, d —back side) VARTM composite laminates.

layer depths of the ballistically impacted laminates. Ultrasonic C-scans for the CMRTM and the VARTM laminates are shown in Fig. 6, which indicate that evolution of the ballistic damage is identical in both the laminate types. The local variations in microstructure (crimp angle, fiber undulation and resin agglomeration) did not affect the ballistic performance of the composites.

4.2. Processing of integral armor

The integral armor was processed using multi-step hand lay-up assist VARTM technique which was subsequently refined to a two step process including single-step VARTM infusion of all layers, followed by secondary bonding of the S2-glass/phenolic fire resistant laminate liner.

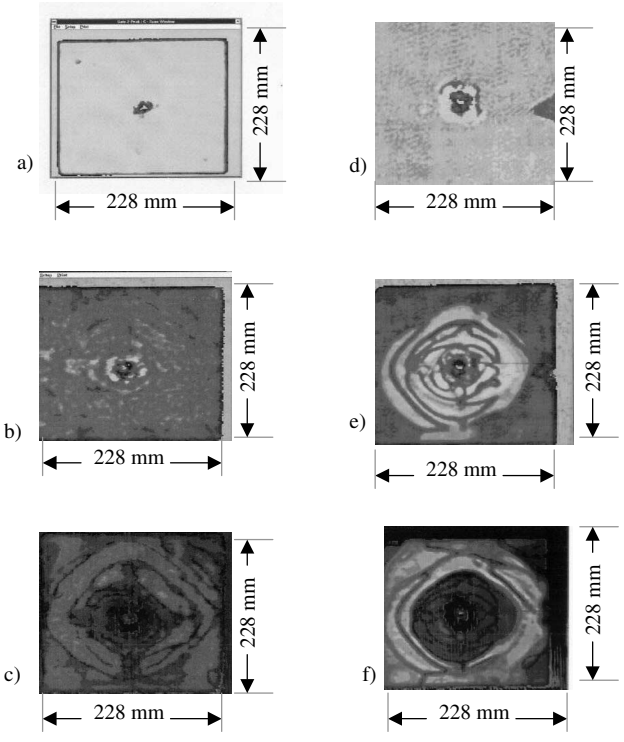

Fig. 6. Layerwise C-scans for ballistic impact damage: (a–c) CMRTM and (d–f) VARTM laminates. Note: a,b — near impact face; c,d — mid-plane of laminate; and e,f — near back side.

4.3. Multi-step hand lay-up assist VARTM technique

The various steps of the operation involved: (a) *Preparation of the rubber layer*. EPDM rubber sheet (3 mm thick) was abraded with 600 grit sand paper on both sides. The sheet was cleaned with acetone. A thin layer of primer was applied to the rubber sheet for preparation of the side for bonding to the ceramic and the S2-glass preform. A layer of E-glass scrim cloth separated each interface. (b) *Preparation of ceramic tiles*. Hexagonal alumina ceramic tiles were cleaned with acetone and wetted with a highly compliant epoxy resin. A thin layer of primer was applied to all the edges of the tile. (c) *Resin infusion of the durability cover*. Six layers of preform for the durability cover (S2-glass layers) were laid over a mold. The hexagonal tiles were placed with small gaps (approximately 0.5 mm apart). The rubber was placed over the ceramic tiles. A vacuum bag was applied and the preform (with ceramic tiles and rubber inclusive) was debulked for about 2 h. Resin was then infused through the preform to obtain the durability cover. The part was then stripped off the bag. (d) *Resin infusion of the thick-section composite*: Forty-five layers of S2-glass, twill weave fabric were laid over the rubber side of the part (containing durability cover, ceramic tiles and rubber) and bagged. Vinyl ester VE-350 resin was then infused through the preform to produce the thick-section composite. (e) *Bonding of lay-up to emi mesh and phenolic liner*. The cured thick structural composite side of the part was lightly sanded, and bonded to an EMI screen which was sandwiched between two E-glass layers. An E-glass/phenolic laminate, 3.18 mm thick, was sanded on one side with a 600 grit sandpaper to provide a bonding surface and then cleaned with acetone. An epoxy paste adhesive was used to

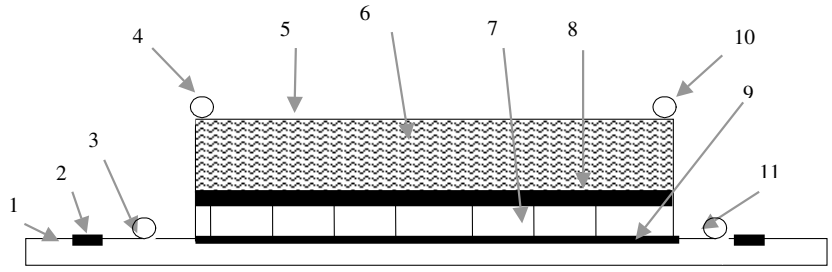

1 Caul Plate. 2 Edge Sealing Tacky Tape. 3 Resin Inlet for Bottom-Side Wetting. 4 Main Resin Inlet for Top-Side Wetting. 5 Resin Distribution Media. 6 Structural Laminate Preform. 7 Ballistic Grade Ceramic Tile. 8 EPDM Rubber. 9 Durability Cover Layers. 10 Top-Side Vacuum. 11 Bottom-Side Vacuum.

Fig. 7. Layout of VARTM processing of integral armor.

bond the S2-glass/epoxy liner to the EMI mesh and the thick-section part all pressed in a pneumatic press to obtain the armor plate. The part was then trimmed on a Felker tile saw with a diamond blade.

4.4. Two-step process: single-step VARTM and secondary bonding of glass/phenolic liner

A revised version of the process was developed such that the entire operation was reduced to a two-step operation. A typical layup is shown in Fig. 7. The process followed the sequence as follows: (a) Six layers of S2-glass preform were laid on the tool, (b) hexagonal ceramic tiles were placed over the perform. A finite gap of 0.50 mm was maintained between each tile, (c) EPDM rubber strips of 50 mm width were placed over the ceramic tiles. A gap of 0.50 mm was maintained between the strips, (d) forty-five layers of S2-glass perform and the EMI mesh were laid over the rubber strips. An E-glass scrim cloth was placed at each interface (rubber–ceramic, rubber–S2-glass and ceramic–S2-glass). The scrim cloth assists in distributing resin between the layers. The part was bagged for VARTM processing. The lay-up was debulked for four hours, prior to resin infusion. Resin was infused in an end-to-end (infusion line at one end of the perform, and the vacuum line at the other end) to fill up the durability cover (the S2-glass) layers which were closest to the caul plate, and hence called bottom-side. Infusion was stopped to the durability cover layers upon its wet-out. Resin was subsequently infused to the top side (to the forty-five structural laminate forming S2-glass perform layers). The process described to bond the glass/phenolic liner was then repeated for secondary bonding. Table 3 provides a breakdown of the processing step and times for the operation steps described using the two approaches for a part size of 76 cm × 50 cm indicating a 36% time savings in adopting the latter approach.

Table 3
Integral armor processing

Step	Number of hours	
	Multi-step hand lay-up assist VARTM	Two-step process
Preparation of rubber layers	2	2
Fabric cutting	2	2
Preparation of ceramic layers	3	3
Constituents lay-up	2[a] 3[b]	2
Bagging time and set-up for infusion	3[a] 3[b]	3
Processing time[c]	5[a] 5[b]	5
Preparation and bonding of phenolic liner	2	2
Total	30	19

[a] Durability cover, signature layer, ceramic tiles and rubber processing.
[b] Thick section composite processing.
[c] Includes cure time.

4.5. Physical property measurements

The panels were measured for their fiber volume fraction and finished thickness. The S2-glass fiber density value was 2.49 gm/cc, and vinyl ester density value of 1.09 gm/cc. The average thickness of the thick-section composite laminated was measured to be 21 mm. The average fiber volume fractions of the laminates ranged between 48–52%. The void content of the laminate part of the thick-section armor was less than 1% (as measured through the burn-off test). Also see Table 4.

The processing integrity of various interfaces of the integral armor was evaluated by SEM. Fig. 8(a)–(d) represent the interface of the durability cover-ceramic tile, the ceramic tile-rubber interface, the rubber-structural composite interface and the structural composite-EMI, and the

Table 4
Average physical properties measured for the armor plates

Weight (kg)	Areal density (kg/m^2)	Dimensions (cm)	Volume fraction[a]	Weight fraction[a]
11.5	123	38 × 26 × 14	48–52%	62%

[a] Volume and weight fractions of the thick composite laminate of the armor.

phenolic laminate interfaces. As can be seen from Fig. 8(a)–(d), distinct interface zones between the dissimilar layers were observed. The bond integrity was found to be uniform through the section of integral armor part.

4.6. Process sensing: flow and cure monitoring

A DC-based sensing technique monitors the flow and cure information, thereby providing a 'window' into the process. A sensor grid, which comprises two orthogonal sets ('sensing' and 'excitation' lines) of conductive filaments separated by one or more preform layers, are placed between layers of the preform. As resin wets the perform during the infusion process, the gaps between the filament planes are filled with conductive resin, which completes an electrical circuit. Associated instrumentation detects the signal and can infer the resin location and cure state.

The sensors adopted in this work were copper wires (0.2 mm in diameter) insulated with E-glass fiber. The sense lines and excitation lines were woven in a glass cloth referred to as 'scrim cloth' to form a sensor mat that could be placed at the interfaces of the various layers, and in the preform of the structural laminate forming layers.

The lay-up for processing consisted of durability cover layers, ceramic tiles, EPDM rubber and structural laminate forming layers as organized from the caul plate side. A layer of E-glass scrim cloth was used to separate each interface. Of these, one infusion line was placed on the top-side of the lay-up (Fig. 7), while the second line was located on the bottom-side, at one of the edges of durability cover layers. The top and bottom sides were wet-out using an end-to-end infusion-vacuum scheme. Distribution meshes were placed at the bottom of the lay-up as well as the top most position in the lay-up. The bottom side mesh was designed to carry the resin to the bottom layers (the durability cover), while the top-side mesh to spread the resin into the S2-glass layers forming the structural laminate. Resin infusion was delayed at the top-side such that the durability layers (bottom side) were wet-out first. It was expected that the resin during its course of wet-out of the durability cover layers, would simultaneously channel through the gaps in the tiles. On observing the resin emerging from the vacuum line of the bottom-side, infusion was started on the top-side of

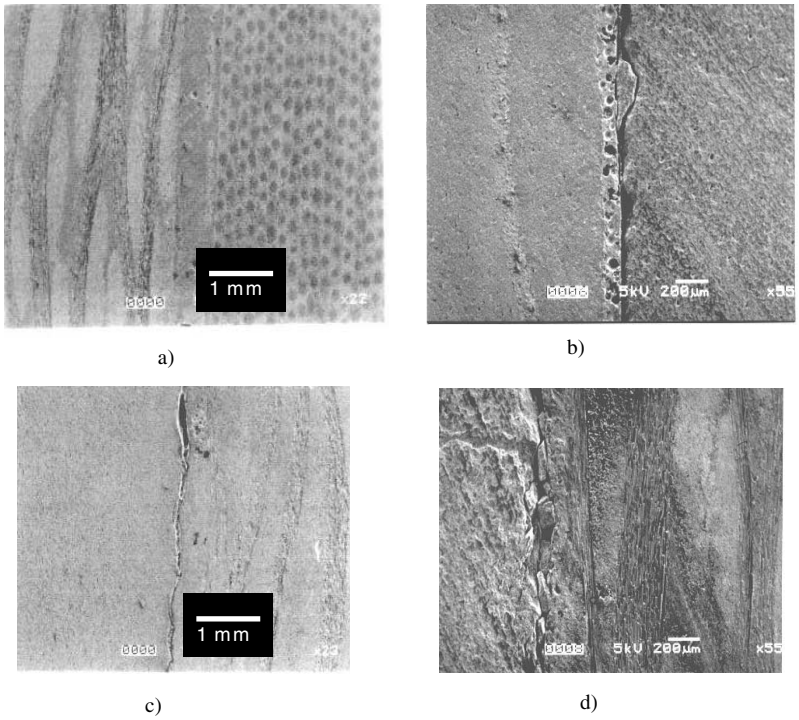

Fig. 8. Microstructure of Armor Interfaces. (a) Phenolic liner-EMI-structural laminate, (b) ceramic–rubber, (c) rubber-structural laminate, and (d) ceramic–rubber-structural laminate.

the lay-up. Four planes of excitation and sense lines (grid of 4×4) were used at the interfaces between the durability cover and ceramic tile, the ceramic tile and EPDM rubber, rubber and S2-glass perform (making up the structural laminate), and at the center of the S2-glass preform.

Fig. 9(a)–(f) depicts the flow of resin at various interfaces of the integral armor during the VARTM process. Each figure (a)–(f) shows results from the four planes of sensors. The presence of resin is sensed by the increase in voltage at the respective grid. Typical voltage signals shown in Fig. 10(a) and (b) indicate the arrival of resin at a grid junction and the onset of resin cure, respectively. From Fig. 9(a), it may be observed that as the resin started flowing at the bottom-side distribution mesh, it simultaneously progressed through the gaps between ceramic tiles (time frame 815 s). As resin reached the interface between the ceramic–rubber, it started flowing rapidly. As only E-glass scrim cloth separates this interface, minimal resistance is offered at this interface, the speed of the resin flow is faster, as compared to the durability cover layers–ceramic tile interface. As seen from Fig. 9(b), the resin wet-out nearly 75% of ceramic–rubber interface, while it had just reached 25% of durability cover layers–ceramic interface. In the latter interface, resin flows through the S-2 glass fabric on its lower side, and the ceramic tiles on its upper side.

After 1290 s (Fig. 9(b)) the entire ceramic–rubber interface was wet-out, and half of the durability cover layers–ceramic interface were wet. The resin traveled through the small gaps on either side of ceramic tiles After 2048 s (Fig. 9(c)) it was observed that both the interfaces were wet, which indicates that resin has traveled through the durability cover layers, and through the ceramic tiles, but was yet to reach the rubber-thick laminate producing S2-glass fabric layers. After 2947 s (Fig. 9(d)) resin enters through the gaps in the rubber strips into the thick composite laminate interface. At the same time frame, the resin was seen to arrive at the bottom-side vacuum line. At this point bottom side (durability cover side) infusion was stopped, and the

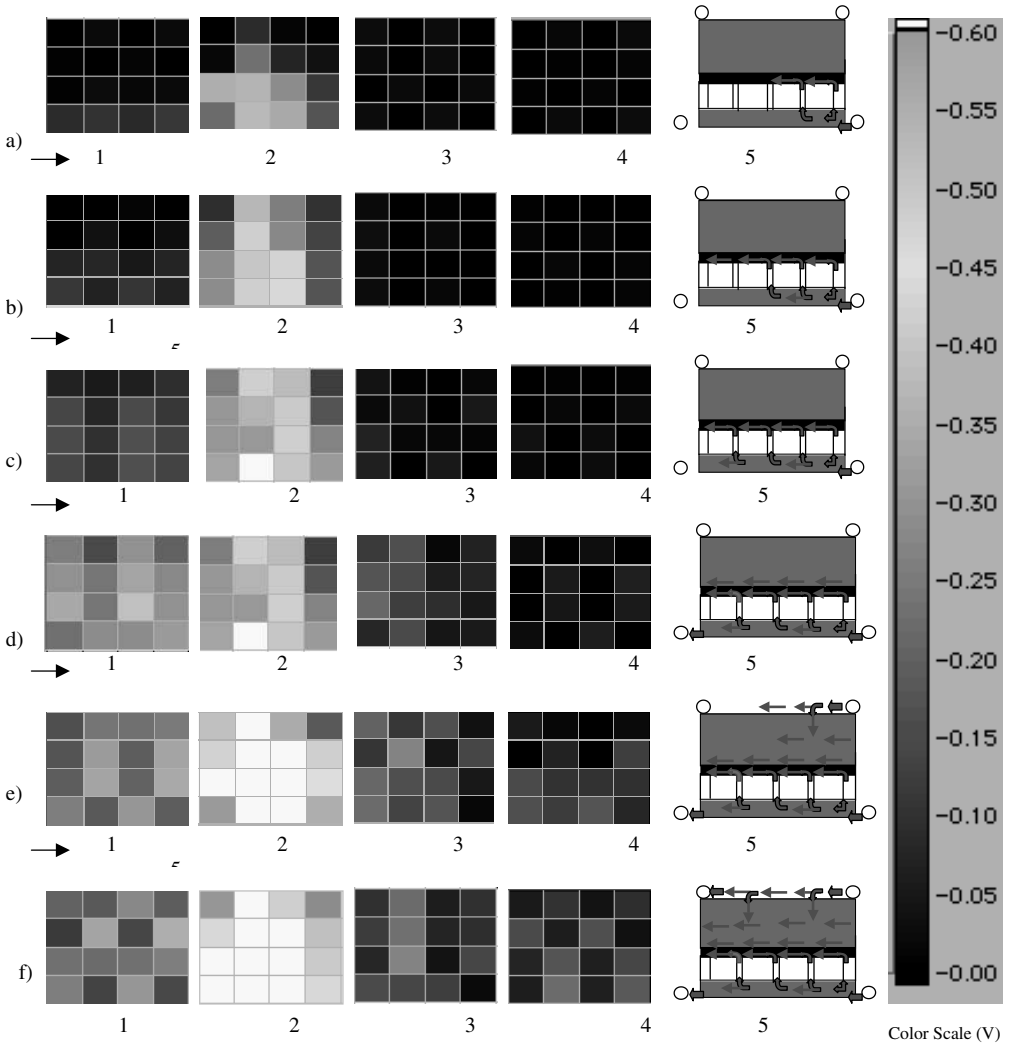

Fig. 9. DC-based sensing of resin flow at various interfaces of the integral armor during the VARTM process. (a) 815 s, (b) 1290 s, (c) 2048 s, (e) 2947 s, and (f) 5067 s.

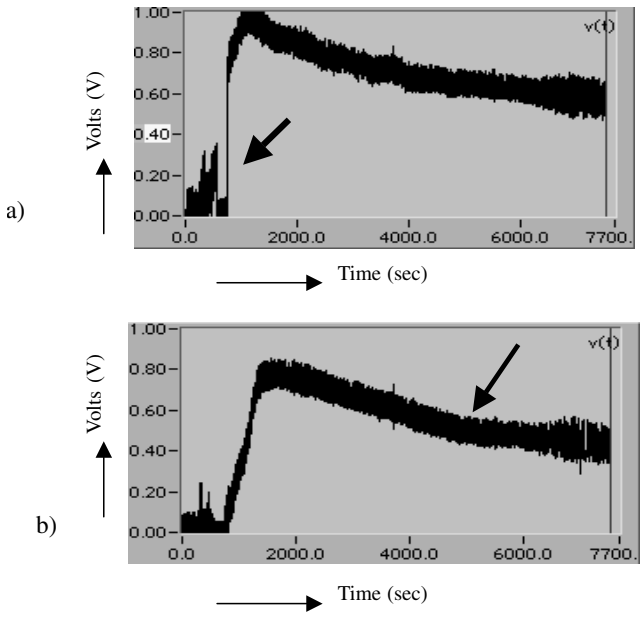

Fig. 10. Representative plots showing voltage of the signals at individual excitation lines. (a) Arrival of resin sensed (increase in voltage, and (b) resin curing starts (dropping of the voltage).

top-side vacuum lines were opened. Resin then flowed through the top-side injection line. The resin infusion lines on the top-side were sequentially activated as resin arrived at the respective infusion line. After 5067 s (Fig. 9(e)) resin was seen to nearly half of center of thick section composite. The entire panel was wet-out after 6303 s (Fig. 9(f)). The voltages diminish as a function of time indicating onset of gelation, and stabilize when the resin begins vitrification.

5. Conclusions

1. Thick S2-glass/vinyl ester composite panels representative of their usage in an integral armor were fabricated using low cost CMRTM and VARTM liquid molding processes.
2. The microstructure measured in terms of crimp angle and weave amplitudes was influenced according to the compaction pressures the preform was subjected to; the CMRTM panels showed 12–14% lower crimp angles as compared to the VARTM panels.
3. Process-related variations arising from a collection of factors including local fiber volume fraction and fabric crimp influenced the static compression and high strain rate impact performance. The CMRTM composites were seen to exhibit higher static compression and high strain rate impact values (5–8%) as compared to the VARTM composite samples.
4. In the case of ballistic impact performance, the processing technique used did not affect the extent of damage. If ballistic performance, is the primary design requirement, the VARTM processing offers an affordable alternative.
5. Composite integral armor panels were manufactured through liquid molding processing techniques. The two-step processing approach resulted in ~36% time savings to produce identical integral armor part as compared to a multi-step VARTM process
6. The DC-based sensing technique provided an insight into the flow and cure of the resin through the various layers of the integral armor part.

Acknowledgements

The support provided by the Army Research Office (ARO) under the Grant No. DAAH04-95-1-0369 is gratefully acknowledged. Assistance from Dr John Gillespie Jr, University of Delaware, Center for Composite Materials (UD-CCM), and Dr Bruce Fink, Army Research Laboratory (ARL) is hereby acknowledged.

References

[1] Burns BP, Hoppel CPR, Newill JF, Burton LW, Tzeng JT, Bender JM, Drysdale WH. An Army perspective on composite materials. In: Whitney JM, editor. Proceedings of the 14th Technical Conference of the American Society for Composites, September. 1999. p. 223–32.
[2] Fink BK. Performance metrics for composite integral armor. In: Whitney JM, editor. Proceedings of the 14th Technical Conference of the American Society for Composites, September. 1999. p. 252–64.
[3] Pike T, McArthur M, Schade D. Vacuum assisted resin transfer molding of a layered structural laminate for application on ground combat vehicles. In: Proceedings of the 28th International SAMPE Technical Conference, November 04-07, Seattle, 1996; 374–80.
[4] Faiz R. Net RTM preforming process for cost-effective manufacturing of military ground vehicle composite structures. In: Proceedings of the 28th International SAMPE Technical Conference, November 04-07, Seattle, WA, 1996; 381–92.
[5] Vaidya UK, Abraham A, Mohamed H, Fotedar K, Haque A, Krishnagopalan J, Mahfuz H, Jeelani S. Manufacturing of composite integral armor using liquid molding processes. In: Green JE, Beckwith SW, Strong AB, editors. Proceedings of the 29th International SAMPE Technical Conference, vol. 29. 1997. p. 523–31.
[6] Bradley JE, Fink BK, Gillespie Jr JW. On-line process monitoring and analysis of large thick-section composite parts utilizing SMARTweave in-situ sensing technology. In: Proceedings of the 43rd International SAMPE Symposium/Exhibition: Materials and Process Affordability-Keys to the Future, SAMPE, Covina, CA, 1998.
[7] England KM, Fink BK, Gillespie Jr JW. In situ sensing of viscosity by direct current measurements. In: Moon TJ, editor. Processing and manufacturing of advanced materials and structures, ASME International Mechanical Engineering Congress and Exposition 1996.
[8] Vaidya UK, Jadhav NC, Hosur MV, Gillespie Jr JW, Fink BK. Assessment of flow and cure monitoring using direct current and alternating current sensing in vacuum assisted resin transfer molding. Smart Materials and Structures 2000;9:727–36.
[9] Rigas EJ, Mulkern TJ, Nguyen SP, Walsh SM, Granville D. Affordable thick composite processing for army applications. In: Whitney JM, editor. Proceedings of the 14th Technical Conference of the American Society for Composites, September. 1999. p. 242–51.
[10] Davis JG. Compression strength of fiber reinforced materials.

Composite reliability, ASTM STP 580ASTM Philadelphia: American Society for Testing Materials, 1975. p. 364–77.

[11] Camponeshi Jr ET. Compression testing of thick-section composite materials. In: O'Brien TK, editor. Composite materials: fatigue and fracture, STP 1110, vol. 3. ASTM Philadelphia: American Society for Testing Materials, 1991. p. 439–56.

[12] Haque A, Ali M, Vaidya UK, Mahfuz H, Jeelani S. Rate dependent compressive response of S2-glass/vinylester composites. In: Green JE, Beckwith SW, Strong AB, editors. Proceedings of the 29th International SAMPE Technical Conference, vol. 29. 1997. p. 698–712.

[13] Hosur MV, Vaidya UK, Abraham A, Jadhav N, Jeelani S. Static and high strain rate compression response of thick section twill weave S2-glass vinyl ester composites manufactured by affordable liquid molding processes. ASME J Engng Mater Technol 1999;121(4):468–75.

[14] Bernetich KR, Fink BK, Gillespie Jr JW. Ballistic testing of affordable composite armor. In: CD-ROM Proceedings of the American Society for Composites 13th Technical Conference, Baltimore, MD, September 21–23, 1998.

[15] Monib AM, Gillespie Jr JW. Damage tolerance of composite laminates subjected to ballistic impact. In: Proceedings of ANTEC 98, Soc. of Plastics Engineers, Brookfield, CT. 1998; 1463–67.